Bull. Chem. Soc. Ethiop. **2024**, 38(1), 213-228.
DOI: https://dx.doi.org/10.4314/bcse.v38i1.16
ISSN 1011-3924
Printed in Ethiopia
Online ISSN 1726-801X

BIOGENIC SYNTHESIS OF SILVER NANOPARTICLES USING ESSENTIAL OIL OF AERIAL PART OF *Cyclospermum leptophyllum* AND THEIR APPLICATION IN COLORIMETRIC DETERMINATION OF METALLIC IONS

Yilma Hunde Gonfa[1,2,4], Mesfin Getachew Tadesse[1,3*], Samuel Abicho Kabeto[1,2], Fekade Beshah Tessema[1,3,5], Archana Bachheti[6], Kundan Kumar Chaubey[7] and Rakesh Kumar Bachheti[1,2,8]

[1]Department of Industrial Chemistry, College of Natural and Applied Sciences, Addis Ababa Science and Technology University, Addis Ababa, Ethiopia
[2]Nanotechnology Centre of Excellence, Addis Ababa Science and Technology University, Addis Ababa, Ethiopia
[3]Biotechnology and Bioprocessing Centre of Excellence, Addis Ababa Science and Technology University, Addis Ababa, Ethiopia
[4]Department of Chemistry, College of Natural and Computational Sciences, Ambo University, Ethiopia
[5]Department of Chemistry, College of Natural and Computational Sciences, Woldia University, Ethiopia
[6]Department of Environment Science, Graphic Era University, Dehradun, India
[7]Divisions of Research and Innovation, School of Applied and Life Sciences, Uttaranchal University, Arcadia Grant, P.O. Chandanwari, Premnagar, Dehradun, Uttarakhand-248007, India
[8]Department of Allied Sciences, Graphic Era Hill University, Society Area, Clement Town, Dehradun 248002, India

(Received December 5, 2022; Revised June 23, 2023; Accepted October 16, 2023)

ABSTRACT. The focus of this research was to synthesize biogenic silver nanoparticles (AgNPs) using the essential oil of the aerial part of *Cyclospermum leptophyllum* (CLEO) and investigate their colorimetric determination of metallic ions. In the synthesis of CLEO mediated AgNPs (CLEO-AgNPs), the one-factor-at-a-time method was used to optimize the reaction parameters. Ultraviolet-visible (UV-Vis) peak of CLEO-AgNPs was determined at 426 nm. Fourier transform-infrared (FTIR) spectra analysis identified the functional groups participating in the bio-reducing, capping, and stabilizing processes in the CLEO-AgNPs synthesis. Scanning electron microscope (SEM) image demonstrated the predominately spherical shape and the average size of 70.86±1.80 nm of CLEO-AgNPs. Energy dispersive X-ray spectroscopy (EDX) peak profile depicted the presence of Ag elements in CLEO-AgNPs. The X-ray diffraction (XRD) peaks observed at 38.5°, 44°, 65°, and 77° which represent Ag(111), Ag(200), Ag(220), and Ag(311) lattice faces, respectively. The average zeta nanosize, zeta potential, and polydispersity index of CLEO-AgNPs were determined as 69.70 nm, -43.5 mV, and 0.256, respectively. The stability test exhibited the prolonged storage stability of CLEO-AgNPs for over six months at room temperature. CLEO-AgNPs demonstrated the potential colorimetric detection of K^+, Mg^{2+}, Al^{3+}, Cr^{6+}, Mn^{2+}, Fe^{3+}, Ni^{2+}, Cu^{2+}, Zn^{2+}, Hg^{2+}, Pb^{2+}, and Cd^{2+} ions in the real samples.

KEY WORDS: *Cyclospermum leptophyllum*, Essential oil, Biogenic silver nanoparticles, Bio-reductants, Colorimetric detection

INTRODUCTION

Currently, the application of noble metal nanoparticles (MNPs) in different areas of application has attracted the interest of several researchers [1]. Nano-dimensions of metals have the interesting physicochemical properties than their bulk counterparts because of their enhanced

*Corresponding author. E-mail: mesfin.getachew@aastu.edu.et

surface area and optical, electronic, catalytic, and biological properties [2, 3]. AgNPs highly attract the interest of many scholars as a result of their extraordinary properties such as conductivity, stability, and wide applications in bio-labelling characteristics, sensors, drug delivery, food industries, wound healings, water purifications, catalysis, paints, agriculture, and cosmetics [1, 4, 5]. AgNPs also showed potential applications in the textiles and electronics industries [6]. AgNPs are one of the early prepared and most vital MNPs because of their characteristic localized surface plasmon resonance (LSPR) spectra absorption in the ultraviolet-visible region of electromagnetic radiation [7].

Plant-assisted AgNPs synthesis is an emerging, developing, and attractive approach over other methods of AgNPs synthesis due to its minimum cost, environmentally friendly, low-toxicity, and biodegradability approach [8]. Plant secondary metabolites are known for their source of bioactive compounds with potential reducing and capping applications for the Ag^{+} ions and AgNPs, respectively [9, 10]. Essential oils (EOs) from the stem, aerial part, leaf, fruit, bark, seeds, and root utilize in different applications [11]. For instance, EOs are classes of natural products with interesting applications in forming MNPs due to their diversified functional groups [12-14]. Therefore, chemical constituents of EOs are potent bio-reducing agents in synthesizing safe, economical, and eco-friendly AgNPs [15]. Some earlier research findings also revealed that EOs were applied as potential bio-reducing agents for converting Ag^{+} ions into Ag^{0} in AgNPs [16]. The increasing of research interest in biogenic AgNPs synthesis and its uses in the biological, agricultural, and medical sectors is because of their high biocompatibility property [17]. Biogenic AgNPs have a significant application in the areas of antimicrobial activities, colorimetric determination of metal ions, agriculture productivity, catalytic reduction activity, textile industry and water purification [18, 19].

Cyclospermum leptophyllum (Pers.) Sprague ex Britton & P. Wilson, family Apiaceae, is a traditional medicine used to heal mild balm, stomachache, and diarrhea disorders [20]. This plant species is an indigenous plant to Ethiopia. Phytochemical investigation of EOs of *C. leptophyllum* with their potential biological activity evaluation was reported with promising results [21, 22]. The main reason for selection of *C. leptophyllum* for the study was to synthesize AgNPs using EO of the plant species and investigate their potential colorimetric probe of metal ions. Previously, there was no research report on the *C. leptophyllum* mediated AgNPs synthesis and study of their potential application. These findings might provide important scientific information to scholars about this medicinal plant-mediated AgNPs synthesis and their promising activity in the colorimetric detection of metal ions in the future. Therefore, this research aimed to isolate EO from the aerial part of *C. leptophyllum* (CLEO), synthesize CLEO mediated AgNPs, and finally investigate the potential colorimetric determination of K^{+}, Mg^{2+}, Al^{3+}, Cr^{6+}, Mn^{2+}, Fe^{3+}, Ni^{2+}, Cu^{2+}, Zn^{2+}, Hg^{2+}, Pb^{2+}, and Cd^{2+} ions using CLEO-AgNPs.

EXPERIMENTAL

Plant sample collection, authentication, and preparation

C. leptophyllum was collected from Tullu Dimtu, Addis Ababa, Ethiopia, situated at the latitude of 8° 88′ North and longitude of 38° 80′ East, an elevation of 2143 m, in November 2020. The plant species authentication was done by Mr. Melaku Wondafrash, Department of Plant Biology and Biodiversity Management, College of Natural and Computational Sciences, Addis Ababa University, and deposited with voucher specimen YH21 at the National Herbarium, AAU, Addis Ababa, Ethiopia. The plant's aerial part was cleaned and dried carefully under shade for two weeks. The dried plant sample was ground to a fine powder using the electric grinder and stored in a non-transparent glass bottle until further analysis.

Chemicals

All chemicals used for the experiments were of analytical grade and purchased from Sigma-Aldrich (St. Louis, Missouri, USA) agents. The preparation of all test solutions was performed using distilled water.

Essential oil extraction

The powder sample of aerial part of *C. leptophyllum* (2 kg) was subjected to hydrodistillation process in a Clevenger-type apparatus for 3 h based on the procedure reported by Pande *et al.* [23]. Then, the extracted essential oil (CLEO) was separated and dried over anhydrous Na_2SO_4 from the aqueous phase and finally, it was stored at the temperature of 4 ^oC until the next experiment.

Essential oil composition analysis

The analysis of chemical composition of CLEO was performed using GC-MS techniques according to the procedure reported by the previous literature report [20]. GC-MS analysis (Thermo Fisher Scientific Inc., Waltham, MA, USA) was carried out using a Varian CP-3800 gas-chromatograph equipped with a DB-capillary column (30 m x 0.25 mm coating thickness 0.25 μm) and a Varian Saturn 2000 ion trap mass detector. The following analytical procedures were used. Injector and transfer line temperatures 220 °C and 240 °C, respectively; oven temperature programmed from 60-240 °C at 3 °C/min; carrier gas helium at 1 mL/min; injection of 0.2 μL (10% hexane solution); split ratio 1:30. The characterization of the chemical compounds of CLEO was performed according to the comparison of the retention times with those of authentic samples and comparing their linear Kovat's indices (KIs) relative to the series of n-alkanes (C_7-C_{25}), NIST database, and Wiley libraries.

Optimization of the synthesis of CLEO-AgNPs

The optimization of reaction conditions for CLEO-AgNPs synthesis was performed according to the earlier literature study [16] with some minor modifications. While keeping the other factors constant, the one-factor-at-a-time variation method was used for the optimization of reaction parameters during the synthesis of CLEO-AgNPs. In this research work, the influence of various reaction conditions was examined by varying pH of $AgNO_3$ solution at 5, 7, 9, 10, and 11, the concentration of $AgNO_3$ solution at 0.4 x 10^{-3}, 1.0 x 10^{-3}, 2.0 x 10^{-3}, 3.0 x 10^{-3}, 4.0 x 10^{-3}, and 6.0 x 10^{-3} M, the volume of CLEO solution at 15, 20, 25, and 30, reaction temperature at 40, 50, 60, 80, and 90 °C, and reaction time at 20, 30, 40, and 50 min. In the biogenic synthesis process, CLEO solution (1 mL CLEO:170 mL acetone ratio) was added slowly using drop-wise to 70 mL of the boiling $AgNO_3$ solution on the digital hot plate with a magnetic stirrer. Finally, all the determined optimum reaction parameters were utilized for the synthesis of CLEO-AgNPs. The CLEO-AgNPs formation progress was controlled by brown color visualization and UV-Vis spectra analysis.

Characterization of the synthesized CLEO-AgNPs

Characterization of the synthesized AgNPs was performed based on the earlier procedures [8, 15]. FTIR spectroscopy (iS50 ABX, Thermo Scientific, Waltham, MA, USA) was employed for the characterization of functional groups of chemical constituents of CLEO and their activity on the surface of CLEO-AgNPs. A drop of the sample was applied with a resolution of 4 cm^{-1}, a spectral range of 400 - 4000 cm^{-1}, and the number of scans of 32. The UV-Vis spectra were measured over 300 to 700 nm using a UV-Vis spectrophotometer (JASCO V-770, Tokyo, Japan). $AgNO_3$

solution (3 x 10^{-3} M) was used as a reference to adjust the baseline. To characterize the size, shape, morphology, and elemental composition of the CLEO-AgNPs, SEM-EDX (SSX-550 SEM-EDX, Shimadzu Corp., Kyoto, Japan) were analyzed using Sigma 300 operated at 20 kV. Determination of the crystalline nature of CLEO-AgNPs was carried out by X-ray diffractometer (Philips PW1710; Philips Co., Amsterdam, the Netherlands), with an X-ray tube with a copper target emitting Cu-Kα line with a wavelength of 1.54 Å and Bragg's angle of $30° \leq 2\theta \leq 80°$. CLEO-AgNPs boundaries can be calculated from the Debye-Scherrer equation: $L = K (\lambda/\beta) \cos \theta$, where β is the width of the peak (full-width half maximum), λ is the X-ray wavelength at 1.54178 Å, L is the mean diameter of nanoparticles, θ is the angle between radiation and particle plane, and K is a constant which is considered 1 for cubic structures. Zeta size and zeta potential nano-analyzer (Zetasizer nano ZS; Malvern Instruments, Malvern, UK) were applied to measure the average particle size and surface potential of the CLEO-AgNPs. The samples of CLEO-AgNPs were deliberately stored at two different conditions: 4 °C and room temperature, and their storage stabilities were studied using UV-Vis spectroscopic techniques for six months.

CLEO-AgNPs application to colorimetric determination of metallic ions

Selectivity and sensitivity detection tests were performed according to previously reported procedures [24, 25]. For the investigation of the selectivity of metallic ions, 10 mL of 2.0 x 10^{-3}M solution of Hg^{2+} and other metal ions such as K^{+}, Mg^{2+}, Al^{3+}, Cr^{6+}, Mn^{2+}, Fe^{3+}, Ni^{2+}, Cu^{2+}, Zn^{2+}, Cd^{2+}, and Pb^{2+} were mixed with 10 mL of CLEO-AgNPs (60 µg/mL) solution in the transparent glass vials. Subsequently, the change in color for the mixed solutions was visualized and the absorption spectra were monitored by UV-Vis spectroscopy after an appropriate incubation time. The sensitivity of CLEO-AgNPs towards concentration of Hg^{2+} ions was also examined for different concentrations of Hg^{2+} ions solution in the decreasing order: 2.0 x 10^{-3}, 1.5 x 10^{-3}, 1.0 x 10^{-3}, 0.9 x 10^{-3}, 0.7 x 10^{-3}, 0.5 x 10^{-3} and 0.2 x 10^{-3} M solutions in transparent glass vials. The limit of detection (LOD) of CLEO-AgNPs for the concentration of Hg^{2+} ions was examined by the brown color fading visualization and then controlling the changes using UV-Vis peak absorption for the mixed solutions. In all experiments, the samples were prepared under the same conditions and the tests were performed in triplicate. For both selectivity and sensitivity tests, the images of solutions in the vials were captured using a digital camera.

RESULTS AND DISCUSSION

Chemical constituents of essential oil

The GC analysis showed that the major chemical compositions of CLEO are from monoterpene and sesquiterpene hydrocarbons. From the total extracted EO components, oxygenated monoterpene compounds account for about 92.34% and sesquiterpene compounds represent 4.52% while non-oxygenated hydrocarbons and oxygenated hydrocarbons share 3.95% and 0.57%, respectively. 2,5-Dimethoxy-*p*-cymene (**1**) (87.09%), 2-methoxy-1-methyl-4-(1-methylethyl)-benzene (**2**) (3.09%), 2-methoxy-4-methyl-1-(1-methylethyl)-benzene (**3**) (1.71%), and humulene (**4**) (1.15%) were reported as the first four dominant components of EO constituents with the relative area ≥1.15%.

Optimization of reaction processes

Many recent studies demonstrated that optimization of reaction conditions is important for the rapid, stable, and homogenous formation of NPs with a high product yield [26]. In this study, optimization of pH was conducted by varying the pH of $AgNO_3$ solution at 5, 7, 9, 10, and 11 during the synthesis of CLEO-AgNPs while fixing other parameters unchanged. When changing

the pH of the $AgNO_3$ solution from an acidic to an alkaline medium, the reaction process increases the yield of CLEO-AgNPs formation. The change in concentration of H^+ ions in the reaction medium may be responsible for altering the electronegative state of bio-reduction molecules in reducing Ag^+ ions [27]. At pH 5 (acidic medium), the absence of a UV-Vis absorption peak indicated that CLEO-AgNPs were not synthesized successfully due to the inactivation of reducing and capping agents [28]. At pH 7 and 11, UV-Vis spectra were broadened due to the aggregation of CLEO-AgNPs over their nucleation [29]. Therefore, the optimum pH of $AgNO_3$ solution was obtained as pH 10, which is supported by maximum UV-Vis peak intensity. All reactions were conducted individually at different concentrations of $AgNO_3$ solution such as 0.4 x 10^{-3}, 1.0 x 10^{-3}, 2.0 x 10^{-3}, 3.0 x 10^{-3}, 4.0 x 10^{-3}, and 6.0 x 10^{-3}. The growth rate of yield of CLEO-AgNPs was increased with the increasing concentration of $AgNO_3$ solution up to 4.0 x 10^{-3} M, and then, the peak intensity was decreased at 6.0 x 10^{-3} M (Figures 1a and b).

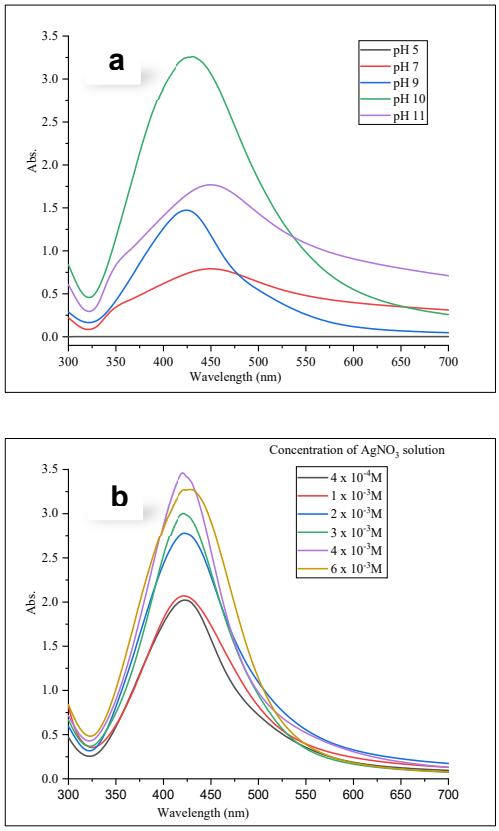

Figure 1. UV-Vis spectra absorption of (**a**) pH and (**b**) concentration of $AgNO_3$ solution optimization process for the synthesis of CLEO-AgNPs.

This effect might be due to the saturation of reactants in the reaction media and caused agglomeration of AgNPs [30, 31], which was observed from the broadening of UV-Vis spectra. Therefore, 4.0 x 10^{-3} M $AgNO_3$ solution was determined as the UV-Vis peak with optimum intensity for CLEO-AgNPs synthesis.

As shown in Figure 2, UV-Vis peak intensity increases as the volume of CLEO solution increases from 15 to 25 mL and then decreases at 30 mL due to the concentrated reducing agents causing the aggregation of the rapid nanoparticles as the formation of larger size CLEO-AgNPs [32]. Therefore, 25 mL of CLEO solution was obtained as the optimum volume of bio-reduction solution for synthesizing CLEO-AgNPs.

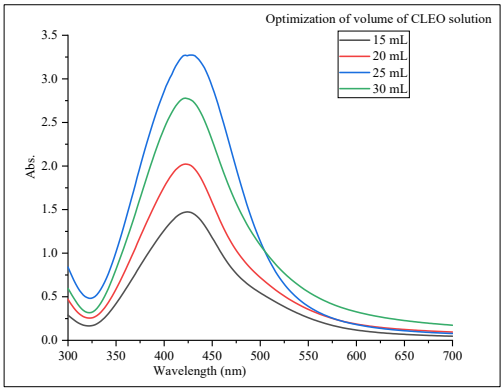

Figure 2. UV-Vis spectra absorption for the optimization of the volume of CLEO solution for the synthesis of CLEO-AgNPs.

The increase in UV-Vis spectra intensity was observed by the increase of reaction temperature from 40 ºC to 80 ºC which might be due to the enhancement of the rate of reaction. At 90 ºC, UV-Vis spectra intensity was decreased due to the lowering effect of the reducing and stabilizing agents [33]. The optimum production of CLEO-AgNPs was obtained at 80 ºC (Figure 3a). UV-Vis spectra intensity was increased with the increase of reaction time from 20 to 40 min and then decreased at 50 min (Figure 3b). Reaction duration influences the rate and yield of biogenic synthesis of AgNPs. This is because of the possibility of aggregation and enlarging the size of synthesized AgNPs at longer time of reaction [34].

Biogenic synthesis of CLEO-AgNPs

CLEO-AgNPs were prepared efficiently at the optimum parameters at pH 10 ($AgNO_3$ solution), 4.0 x 10^{-3} M of $AgNO_3$ solution, 25 mL of CLEO solution, 80 °C, and 40 min. Along with these optimum parameters, 70 mL of $AgNO_3$ solution was used throughout all experiments. The highly responsible bio-reducing, capping, and stabilizing agents for forming CLEO-AgNPs may be 2,5-dimethoxy-*p*-cymene (**1**) which accounts for 87.09% of the total essential oil composition.

Characterization of CLEO-AgNPs

The UV-Vis spectra measurement of CLEO-AgNPs was performed using the UV-Vis spectroscopic technique over a range of 300 to 700 nm (Figure 4a). The observed surface plasmon resonance (SPR) peak in 400-500 nm is the normal UV-Vis absorption range indicating AgNPs formation. The characteristic brown solution resulted from the excitation and collective oscillation of free electrons on the surface of AgNPs that interact with light waves [25, 35]. Hence, the formation of CLEO-AgNPs was determined by brown color visualization and characteristic UV-Vis peak absorption at 426 nm. The broadening of UV-Vis peak of CLEO-AgNPs is more probably due to the aggregation of NPs after their formation [25].

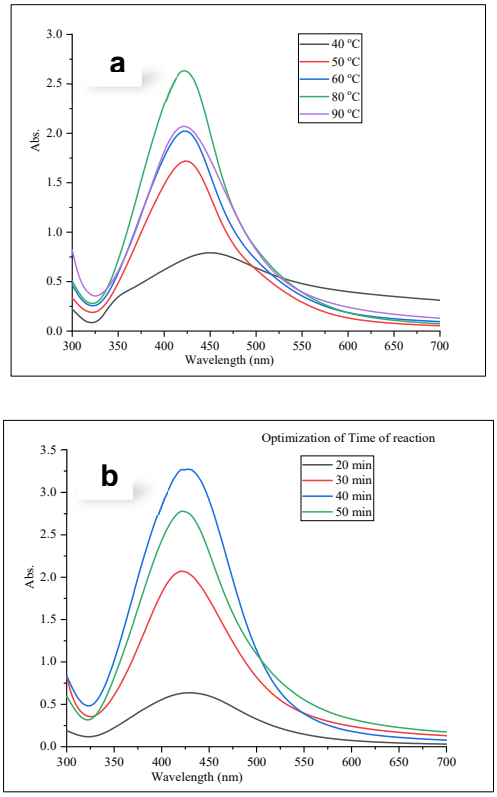

Figure 3. UV-Vis spectra absorption of the (**a**) temperature and (**b**) time of reaction optimization for the synthesis of CLEO-AgNPs.

FTIR results also showed the elimination of some peaks of CLEO and the formation of new peak patterns after CLEO-AgNPs formation (Figure 4b). The major FTIR characteristic peaks of functional groups of chemical constituents of CLEO at 1506, 1465, 1402, 1207, and 1047 cm^{-1} were disappeared and the new peaks were resulted at 3280 cm^{-1} and 1654 cm^{-1} after the synthesis of CLEO-AgNPs. Some studies reported that FTIR analysis determines the functional groups that are used in the synthesis of MNPs as reducing, capping, and stabilizing agents [18]. This has occurred as a result of the oxidation-reduction reaction between functional groups of CLEO chemical constituents and Ag^{+} ions during CLEO-AgNPs synthesis. The change of aromatic ring and C-O groups to -O-H and C=C groups could result from redox reaction [36-38].

From the SEM image, the formation of CLEO-AgNPs was observed with a predominately spherical shape and an average size of 70.86 ± 1.80 nm. EDX profile displayed the presence of Ag elements in the synthesized CLEO-AgNPs. An EDX profile analysis showed a major peak at about 3.0 keV, which indicates the production of Ag element as a result of Ag^{+} ions reduction in AgNPs synthesis [39]. SEM image and EDX profile for CLEO-AgNPs are presented in Figures 5a and b.

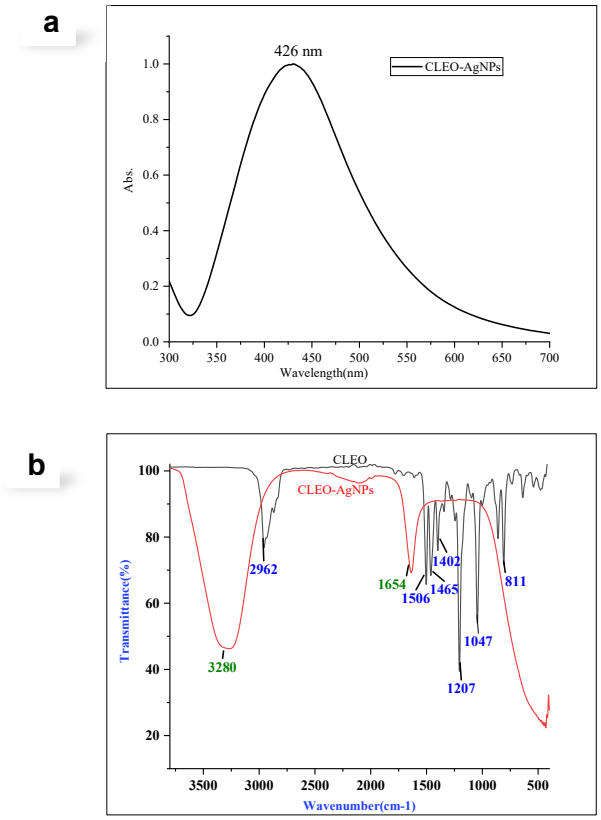

Figure 4. (**a**) UV-Vis spectrum and (**b**) FTIR peaks of the synthesized CLEO-AgNPs.

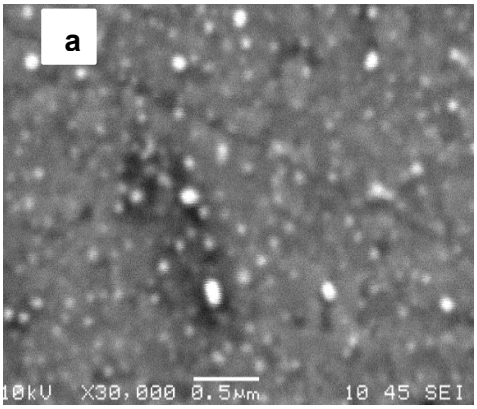

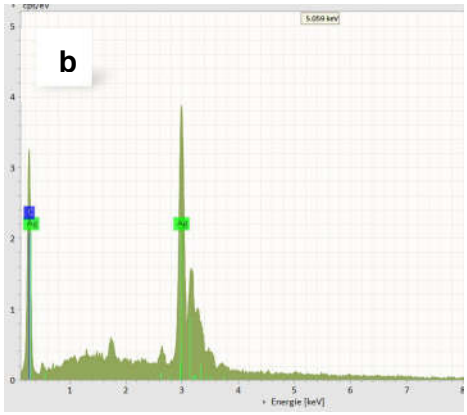

Figure 5. (**a**) SEM image and (**b**) EDX profile for the synthesized CLEO-AgNPs.

As shown in Figure 6, XRD analysis displays characteristic peaks at 38.5°, 44°, 65°, and 77°, which are assigned to Ag (111), Ag (200), Ag (220), and Ag (311) lattice faces, respectively. The XRD pattern demonstrated a consistent agreement with the findings reported in the previous studies with the standard reference JCPDS No. 04-0873 [40]. These XRD peaks indicated that the synthesized CLEO-AgNPs have a face-center cubic crystalline nature. An earlier report on *Chenopodium botrys* aqueous extract mediated AgNPs by Yari and co-workers [41] supports the XRD analysis result in this study.

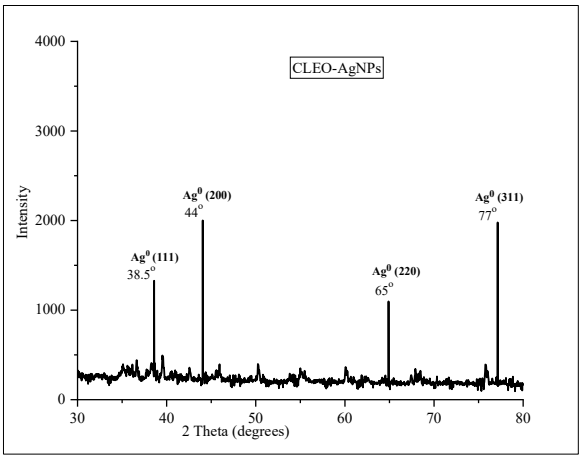

Figure 6. XRD pattern of CLEO-AgNPs.

The existing literature supports the stability of CLEO-AgNPs. The particle size and zeta potential analyzer instruments characterized the average particle size and distribution of CLEO-AgNPs. The measurement of synthesized AgNPs size distribution was shown in Figures 7a and b. The values of the average size (diameter), zeta potential, and polydispersity index (PDI) were

obtained as 69.70 nm, -43.5 mV, and 0.256, respectively for CLEO-AgNPs. Zeta potential measurement of particles by DLS helps to determine the electrostatic attraction or repulsion state between the synthesized AgNPs. Zeta potential values greater than ±30 mV are the indicators of the stability of the synthesized AgNPs in suspension [42]. In the range of 0 to 1, the small value of the polydispersity index (PDI) has been reported to inform the homogeneity of the size of AgNPs [43, 44].

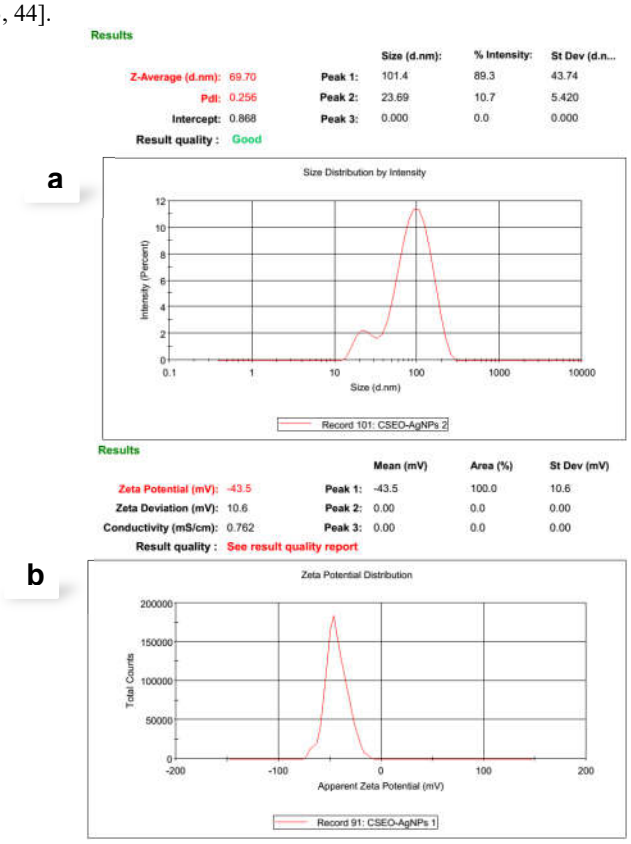

Figure 7. (**a**) Size distribution by the intensity and (**b**) zeta potential of CLEO-AgNPs.

Stability is one of the parameters that ensure the life span of the synthesized AgNPs to be used in various areas of applications effectively [16, 40, 45]. The physicochemical stability of CLEO-AgNPs was studied for six months using UV-Vis spectroscopy (Figures 8a and b).

CLEO-AgNPs sample decreased in yield which confirmed by the SPR UV-Vis peak intensity after one month storage in refrigerator (below 4 °C). However, the storage stability of CLEO-AgNPs was high at room temperature against aggregation almost for over six months.

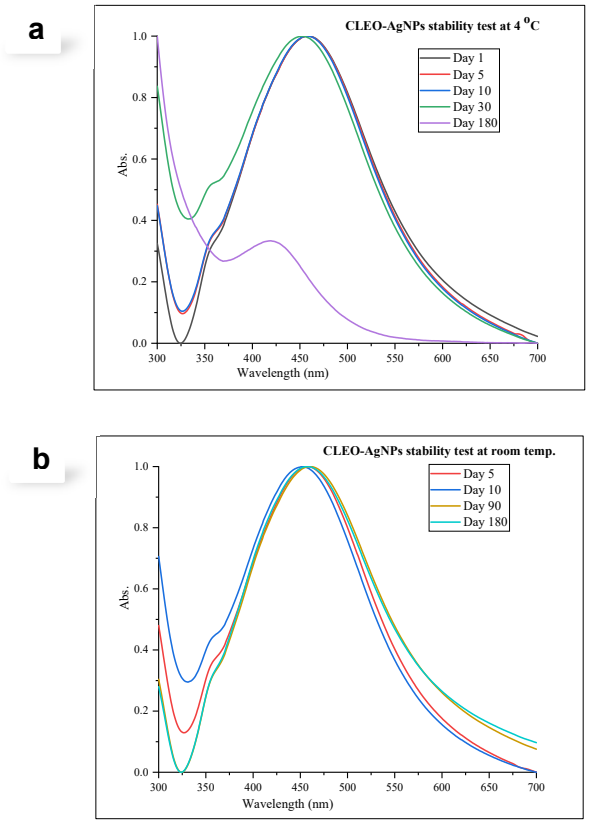

Figure 8. UV-Vis spectra for the stability test of CLEO-AgNPs over six months at (**a**) 4 °C, (**b**) room temperature.

Selectivity and sensitivity tests of the colorimetric determination of metallic ions

Selectivity and sensitivity tests of metallic ions were performed according to the adopted procedure from some previous research reports [7, 24, 25]. CLEO-AgNPs colloidal solution and different metal ions: K^{+}, Mg^{2+}, Al^{3+}, Cr^{6+}, Mn^{2+}, Fe^{3+}, Ni^{2+}, Cu^{2+}, Zn^{2+}, Hg^{2+}, Pb^{2+}, and Cd^{2+} were mixed in transparent glass vials and let to stand for 20 min at room temperature. Then, the disappearance of the brown color of CLEO-AgNPs solution was visualized through the naked eye selectively only to the vial containing Hg^{2+} ions which confirmed the disappearance of the SPR peak at 426 nm (Figures 9a and b). Even though there was no clear visualization of brown color change, UV-Vis spectra analysis demonstrated blue shift and peak narrowing for Cr^{6+} ions and red shift and peak broadening for Al^{3+}, Fe^{3+}, Ni^{2+}, Cu^{2+}, and Pb^{2+} ions upon mixing with the brown CLEO-AgNPs colloidal solution.

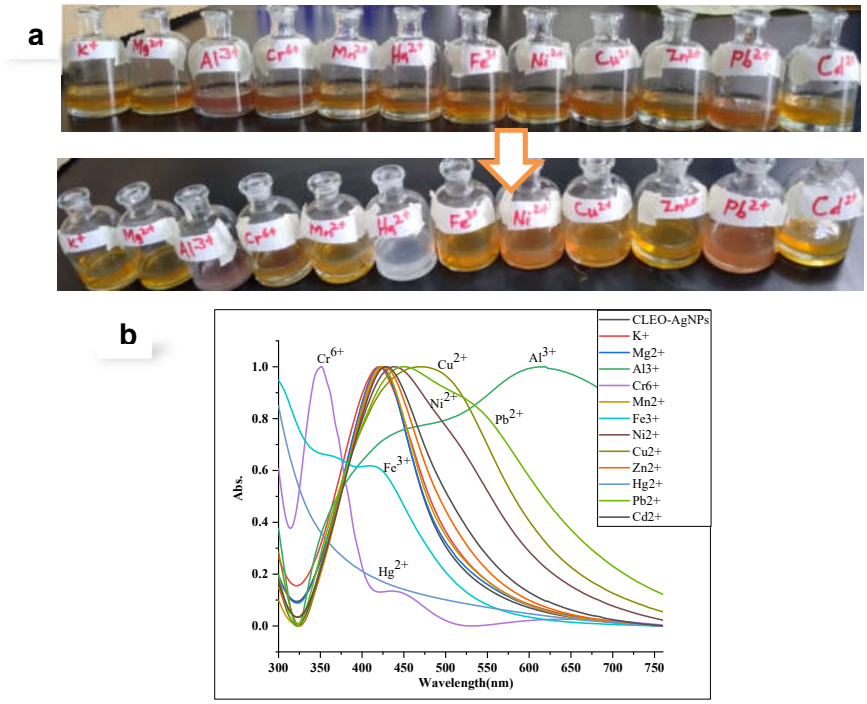

Figure 9. (**a**) Camera image of CLEO-AgNPs- metallic ions mixtures, (**b**) UV-Vis spectra of solutions of various metallic ions and CLEO-AgNPs mixtures.

Therefore, colorimetric detection of CLEO-AgNPs towards various metallic ions demonstrated the strongest selectivity towards Hg^{2+} ions over the other metallic ions. This effect depicts CLEO-AgNPs are highly applied for the qualitative analysis of Hg^{2+} ions in real samples. The electrochemical series approach is used to explain the colorimetric detection mechanism of Hg^{2+} ions due to metals with higher electrochemical reduction potential show greater tendency as oxidizing agents [24]. The disappearance of color and SPR UV-Vis peak of CLEO-AgNPs in the existence of Hg^{2+} ions are a result of the removal of stabilizing agents from the AgNPs and capping Hg^{2+} ions which causes aggregation of AgNPs or oxidation of Ag^0 in AgNPs to Ag^+ ions by Hg^{2+} ions, i.e., dissolution of AgNPs [7]. A further experiment was conducted to investigate how the lower concentration of Hg^{2+} ions can be detected by CLEO-AgNPs solution. Figures 10a and b show the sensitivity test of CLEO-AgNPs solution towards the concentrations of Hg^{2+} ions at 2.0 x 10^{-3}, 1.5 x 10^{-3}, 1.0 x 10^{-3}, 0.9 x 10^{-3}, 0.7 x 10^{-3}, 0.5 x 10^{-3}, and 0.2 x 10^{-3}M. This result reveals that the synthesized AgNPs can detect the minimum concentration of Hg^{2+} ions up to 0.5 x 10^{-3} M.

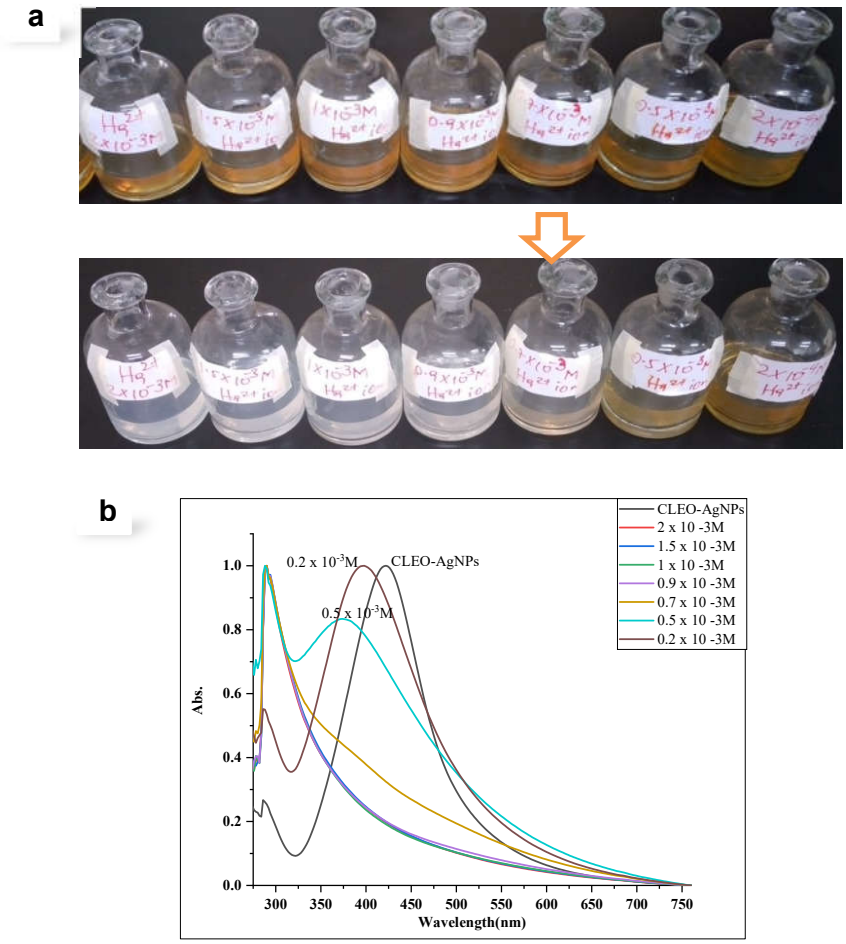

Figure 10. (**a**) Camera image of CLEO-AgNPs and Hg^{2+} ion mixtures, (**b**) UV-Vis spectra of sensitivity test of CLEO-AgNPs towards different concentrations of Hg^{2+} ions.

CONCLUSIONS

In this research work, biogenic AgNPs were prepared successfully based on the cost-effective and non-toxic approach using CLEO. Various reaction conditions were optimized and used for the synthesis of CLEO-AgNPs. UV-Vis, FTIR, SEM-EDX, XRD, and zeta sizer were applied to confirm the AgNPs formation. The characteristic UV-Vis absorption for CLEO-AgNPs was observed at 426 nm. The combined FTIR spectra analysis showed the major functional groups of chemical constituents of CLEO serve as reducing, capping, and stabilizing agents in the formation of CLEO-AgNPs. SEM image analysis determined the shape and average size of CLEO-AgNPs as spherical shape and 70.89 ± 1.80 nm, respectively. The characteristic EDX peak at 3.0 keV depicts the presence of the Ag elements in the CLEO-AgNPs. XRD analysis also showed the characteristic peaks of CLEO-AgNPs at 38.5°, 44°, 65°, and 77°, which are assigned to Ag (111), Ag (200), Ag (220), and Ag (311) crystal lattice, respectively. The average size, zeta potential,

and polydispersity index of CLEO-AgNPs were determined as 69.70 nm, -43.5 mV, and 0.256, respectively. The stability test of CLEO-AgNPs demonstrated the promising storage stability for about six months at room temperature. CLEO-AgNPs demonstrated the strongest selectivity towards Hg^{2+} ions than other metallic ions. Therefore, CLEO-AgNPs exhibited a promising colorimetric probe of Hg^{2+} ions. CLEO-AgNPs displayed medium sensitivity detection towards the concentration of Hg^{2+} ions. However, further study will be required to improve the sensitive detection of CLEO-AgNPs to the minimum possible concentration of Hg^{2+} ions. The future aspect of this study is to extend the usage of extracts of *C. leptophyllum* for the biogenic synthesis of MNPs and widely investigate their potential applications in various fields. In conclusion, the biogenic synthesis approach is a promising alternative to the existing expensive and harmful methods of preparing MNPs for the potent environmental, agricultural, biological, and medical applications.

ACKNOWLEDGEMENTS

The authors acknowledge the helpful assistance from Central Research Laboratories of Addis Ababa Science and Technology University for providing instruments for spectroscopic analysis. We also appreciate Dr. Bekele Hailegnaw and Dr. Getachew Adam for their cooperation in the SEM and EDX analysis of CLEO-AgNPs samples.

REFERENCES

1. Khan, S.; Singh, S.; Gaikwad, S.; Nawani, N.; Junnarkar, M.; Pawar, S.V. Optimization of process parameters for the synthesis of silver nanoparticles from Piper betle leaf aqueous extract, and evaluation of their antiphytofungal activity. *Environ. Sci. Pollut. Res.* **2020**, 27, 27221-27233.
2. Firdhouse, M.J.; Lalitha, P. Biosynthesis of silver nanoparticles and its applications. *J. Nanotechnol.* **2015**, Article ID 829526, 18 pages.
3. Agarwal, H.; Shanmugam, V.K. A review on anti-inflammatory activity of green synthesized zinc oxide nanoparticle: Mechanism-based approach. *Bioorg. Chem.* **2020**, 94, 1-35.
4. Ismail, M.; Khan, M.I.; Khan, S.B.; Akhtar, K.; Khan, M.A.; Asiri, A.M. Catalytic reduction of picric acid, nitrophenols and organic azo dyes via green synthesized plant supported Ag nanoparticles. *J. Mol. Liq.* **2018**, 268, 87-101.
5. Rafique, M.; Sadaf, I.; Rafique, M.S.; Tahir, M.B. A review on green synthesis of silver nanoparticles and their applications. *Artif. Cells Nanomed. Biotechnol.* **2017**, 45, 1272-1291.
6. Ahmed, R.H.; Mustafa, D.E. Green synthesis of silver nanoparticles mediated by traditionally used medicinal plants in Sudan. *Int. Nano Lett.* **2020**, 10, 1-14.
7. Azimpanah, R.; Solati, Z.; Hashemi, M. Green synthesis of silver nanoparticles and their applications as colorimetric probe for determination of Fe^{3+} and Hg^{2+} ions. *IET Nanobiotechnol.* **2018**, 12, 673-677.
8. Shehabeldine, A.M.; Elbahnasawy, M.A.; Hasaballah, A.I. Green phytosynthesis of silver nanoparticles using *Echinochloa stagnina* extract with reference to their antibacterial, cytotoxic, and larvicidal activities. *J. BioNanoSci.* **2021**, 11, 526-538.
9. Aljohny, B.O.; Almaliki, A.A.A.; Anwar, Y.; Ul-Islam, M.; Kamal, T. Antibacterial and catalytic performance of green synthesized silver nanoparticles embedded in crosslinked PVA sheet. *J. Polym. Environ.* **2021**, 29, 3252-3262.
10. Rashmi, V.; Prabhushankar, H.B.; Sanjay, K.R. *Centella asiatica* L. callus mediated biosynthesis of silver nanoparticles, optimization using central composite design, and study on their antioxidant activity. *Plant Cell Tissue Organ Cult.* **2021**, 146, 515-529.
11. Nartey, D.; Gyesi, J.N.; Borquaye, L.S. Chemical composition and biological activities of the essential oils of *Chrysophyllum albidum* G. Don (African Star Apple). *Biochem. Res. Int.* **2021**, Article ID 9911713, 11 pages.

12. Nerio, L.S.; Olivero-Verbel, J.; Stashenko, E. Repellent activity of essential oils: A review. *Bioresour. Technol.* **2010,** 101, 372-378.
13. Asbahani, A.E.; Miladi, K.; Badri, W.; Sala, M.; Addi, E.H.A.; Casabianca, H.; Mousadik, A.E; Hartmann, D.; Jilale, A.; Renaud, F.N.R., Elaissari, A.; Lyon, C.B. Essential oils: From extraction to encapsulation. *Int. J. Pharm.* **2015**, 483, 220-243.
14. Trifan, A.; Luca, S.V.; Greige-Gerges, H.; Miron, A.; Gille, E.; Aprotosoaie, A.C. Recent advances in tackling microbial multidrug resistance with essential oils: Combinatorial and nano-based strategies. *Crit. Rev. Microbiol.* **2020**, 46, 338-357.
15. Yang, N.; Weihong, L.; Hao, L. Biosynthesis of Au nanoparticles using agricultural waste mango peel extract and its in vitro cytotoxic effect on two normal cells. *Mater. Lett.* **2014**, 134, 67-70.
16. Maciel, M.; da Rosa A.A.; Machado, M.H.; Elias, W.C.; Gonçalves da Rosa, C.; Teixeira, G.L.; Noronha, C.M.; Bertoldi, F.C.; Nunes, M.R.; de Armas, D.R.; Barreto, P.L. Green synthesis, characteristics and antimicrobial activity of silver nanoparticles mediated by essential oils as reducing agents. *Biocatal. Agric. Biotechnol.* **2020**, 28, 1-8.
17. Kumar, B. Green synthesis of gold, silver, and iron nanoparticles for the degradation of organic pollutants in wastewater. *J. Compos. Sci.* **2021**, 5, 1-26.
18. Tarannum, N.; Gautam, Y.K. Facile green synthesis and applications of silver nanoparticles: A state-of-the-art review. *RSC Adv.* **2019**, 9, 34926-34948.
19. Salayová, A.; Bedlovičová, Z.; Daneu, N.; Baláž, M.; Lukáčová, B.Z.; Balážová, L.; Tkáčiková, L. Green synthesis of silver nanoparticles with antibacterial activity using various medicinal plant extracts: Morphology and antibacterial efficacy. *Nanomaterials* **2021**, 11, 1-20.
20. Iman, E.H.; Amal, A.G.; Hassan-Elrady A.S. Chemical composition and α-amylase inhibitory activity of *Apium leptophyllum* essential oils. *J. Am. Sci.* **2015**, 11, 1-7.
21. Singh, C.; Singh, S.; Pande, C.; Tewari, G.; Pande, V.; Sharma, P. Exploration of antimicrobial potential of essential oils of *Cinnamomum glanduliferum*, *Feronia elephantum*, *Bupleurum hamiltonii* and *Cyclospermum leptophyllum* against foodborne pathogens. *Pharm. Biol.* **2013**, 51, 1607-1610.
22. Helal, I.; Galala, A.; Saad, H.E.; Halim, A. Bioactive constituents from *Apium leptophyllum* fruits. *Br. J. Pharm. Res.* **2016**, 14, 1-8.
23. Pande, C.; Tewari, G.; Singh, C.; Singh, S. Essential oil composition of aerial parts of *Cyclospermum leptophyllum* (Pers.) Sprague ex Britton and P. Wilson. *Nat. Prod. Res.* **2011**, 25, 592-595.
24. Kalam, A.; Al-Sehemi, A.G.; Alrumman, S.; Assiri, M.; Moustafa, M.F.M.; Yadav, P.; Pannipara, M. Colorimetric optical chemosensor of toxic metal ion (Hg^{2+}) and biological activity using green synthesized AgNPs. *Green Chem. Lett. Rev.* **2018**, 11, 484-491.
25. Ahmed, F.; Kabir, H.; Xiong, H. Dual colorimetric sensor for Hg^{2+}/Pb^{2+} and an efficient catalyst based on silver nanoparticles mediating by the root extract of *Bistorta amplexicaulis*. *Front. Chem.* **2020**, 8, 1-15.
26. Huq, A.; Rahman, M.M.; Balusamy, S.R.; Akter, S. Green Synthesis and potential antibacterial applications of bioactive silver nanoparticles: A review. *Polymers*, **2022**, 14, 1-22.
27. Javed, B.; Nadhman, A.; Mashwani, Z. Optimization, characterization and antimicrobial activity of silver nanoparticles against plant bacterial pathogens phyto-synthesized by *Mentha longifolia*. *Mater. Res. Express* **2020**, 7, 1-13.
28. Sadalage, P.S.; Patil, R.V.; Havaldar, D.V.; Gavade, S.S.; Santos, A.C.; Pawar, K.D. Optimally biosynthesized, PEGylated gold nanoparticles functionalized with quercetin and camptothecin enhance potential anti-inflammatory, anti-cancer and anti-angiogenic activities. *J. Nanobiotechnol.* **2021**,19, 1-17.
29. Ndikau, M.; Noah, N.M.; Andala, D.M.; Masika, E. Green synthesis and characterization of silver nanoparticles using *Citrullus lanatus* fruit rind extract. *Int. J. Anal. Chem.* **2017**, Article

ID 8108504, 9 pages.
30. Arya, G.; Kumari, R.M.; Gupta, N.; Kumar, A.; Chandra, R.; Nimesh, S. Green synthesis of silver nanoparticles using *Prosopis juliflora* bark extract: Reaction optimization, antimicrobial and catalytic activities. *Artif. Cells Nanomed. Biotechnol.* **2018**, 46, 985-993.
31. Hussain, M.; Iqbal R.N.; Iqbal, M.; Aslam, S. Applications of plant flavonoids in the green synthesis of colloidal silver nanoparticles and impacts on human health. *Iran. J. Sci. Technol. Trans. A: Sci.* **2019**, 43, 1381-1392.
32. Patil, S.; Chandrasekaran, R. Biogenic nanoparticles: A comprehensive perspective in synthesis, characterization, application and its challenges. *J. Genet. Eng. Biotechnol.* **2020**, 18, 1-23.
33. Samari, F.; Salehipoor, H.; Eftekhar, E.; Yousefinejad, S. Low-temperature biosynthesis of silver nanoparticles using mango leaf extract: Catalytic effect, antioxidant properties, anticancer activity and application for colorimetric sensing. *New J. Chem.* **2018**, 42, 15905-15916.
34. Liang, M.; Wei, S.; Jian-Xin, L.; Xiao-Xi, Z.; Zhi, H.; Wen, L.; Zheng-Chun, L.; Jian-Xin, T. Optimization for extracellular biosynthesis of silver nanoparticles by *Penicillium aculeatum* Su1 and their antimicrobial activity and cytotoxic effect compared with silver ions. *Mater. Sci. Eng. C,* **2017**, 77, 963-971.
35. Ramdath, S.; Mellem, J.; Mbatha, L.S. Anticancer and antimicrobial activity evaluation of Cowpea-Porous-Starch-Formulated silver nanoparticles. *J. Nanotechnol.* **2021**, Article ID 5525690, 13 pages.
36. Aswathy A.S.; Philip, D. Green synthesis of gold nanoparticles using *Trigonella foenum-graecum* and its size-dependent catalytic activity. *Spectrochim. Acta-Part A:Mol. Biomol. Spectrosc.* **2012**, 97, 1-5.
37. Ayinde, W.B.; Gitari, W.M.; Samie, A. Optimization of microwave-assisted synthesis of silver nanoparticle by *Citrus paradisi* peel and its application against pathogenic water strain. *Green Chem. Lett. Rev*. **2019**, 12, 225-234.
38. Bocsan, I.C.; Pop, R.M.; Sabin, O.; Sarkandy, E.; Boarescu, P.M.; Roşian, Ş.H.; Leru, P.M.; Chedea, V.S.; Socaci, S.A.; Buzoianu, A.D. Comparative protective effect of *Nigella sativa* oil and *Vitis vinifera* seed oil in an experimental model of isoproterenol-induced acute myocardial ischemia in rats. *Molecules* **2021**, 26, 1-18.
39. Saha, J.; Begum, A.; Mukherjee, A.; Kumar, S. A novel green synthesis of silver nanoparticles and their catalytic action in reduction of methylene blue dye. *Sustain. Environ. Res.* **2017**, 27, 245-250.
40. Jain, S.; Mehata, M.S. Medicinal plant leaf extract and pure flavonoid mediated green synthesis of silver nanoparticles and their enhanced antibacterial property. *Sci. Rep.* **2017**, 7, 1-13.
41. Yari, A.; Yari, M.; Sedaghat, S.; Delbari, A.S. Facile green preparation of nano-scale silver particles using *Chenopodium botrys* water extract for the removal of dyes from aqueous solution. *J. Nanostructure Chem.* **2021**, 11, 423-435.
42. Geraldes, A.N.; da Silva, A.A.; Leal, J.; Estrada-Villegas, G.M.; Lincopan, N.; Katti, K.V.; Lugão, A.B. Green nanotechnology from plant extracts: Synthesis and characterization of gold nanoparticles. *Adv. Nanoparticles,* **2016**, 5, 176-185.
43. Yusuf, S.M.; Che Mood, C.A.; Ahmad, N.H.; Sandai, D.; Lee, C.K.; Lim, V. Optimization of biogenic synthesis of silver nanoparticles from flavonoid-rich *Clinacanthus nutans* leaf and stem aqueous extracts: Biogenic synthesis of *C. nutans* AgNPs. *R. Soc. Open Sci*. **2020**, 7, 1-15.
44. Brycki, B.; Szulc, A.; Babkova, M. Synthesis of silver nanoparticles with gemini surfactants as efficient capping and stabilizing agents. *Appl. Sci.* **2021**, 11, 1-14.
45. Sang, S.; Li, D.; Zhang, H.; Sun, Y.; Jian, A.; Zhang, Q.; Zhang, W. Facile synthesis of AgNPs on reduced graphene oxide for highly sensitive simultaneous detection of heavy metal ions. *RSC Adv.* **2017**, 7, 21618-21624.